Effect of sleeper bottom texture on lateral resistance with discrete element modelling

Guo, Yunlong; Fu, Hao; Qian, Yu; Markine, Valeri; Jing, Guoqing

DOI
10.1016/j.conbuildmat.2020.118770

Publication date
2020

Document Version
Accepted author manuscript

Published in
Construction and Building Materials

Citation (APA)
Guo, Y., Fu, H., Qian, Y., Markine, V., & Jing, G. (2020). Effect of sleeper bottom texture on lateral resistance with discrete element modelling. *Construction and Building Materials*, *250*, Article 118770. https://doi.org/10.1016/j.conbuildmat.2020.118770

Effect of Sleeper Bottom Texture on Lateral Resistance with Discrete Element Modelling

Yunlong Guo [1], Hao Fu [2], Yu Qian [3], Guoqing Jing [4*]

1. Faculty of Civil Engineering and Geosciences, Delft University of Technology, Delft, 2628CN, Netherlands
2. Department of Civil Engineering, School of Engineering, University of Birmingham, Birmingham, B152TT, UK
3. Department of Civil and Environmental Engineering, University of South Carolina, Columbia, SC, USA
4. School of Civil Engineering, Beijing Jiaotong University, Beijing, 100044, China
*. Corresponding author
Email addresses: gqjing@bjtu.edu.cn (G. Jing)

Abstract: The lateral stability of ballasted track becomes more important because of the safety requirement under the demand of higher train speed and heavier axle load. To increase the lateral resistance of ballast bed, this paper proposes three types of new sleepers, frictional sleepers. The frictional sleepers are sleepers with different shapes of textures attached at the sleeper bottom. To study the application feasibility of the frictional sleepers, experimental tests (single sleeper pull-out test) and numerical simulation (discrete element modelling) are performed. The lateral resistances of the three types of frictional sleepers are compared with the traditional sleeper based on the experimental test, and the mechanism of the lateral resistance increase is revealed according to the numerical simulation. The results indicate that the frictional sleepers can increase the lateral resistance by 32% (maximum), due to the enhanced interaction between sleeper and ballast particles. More importantly, different types of frictional sleepers have different performances, and the optimal friction sleeper is confirmed. This study is helpful for the further research on sleeper design.

Key words: Fictional sleeper; Lateral resistance; Discrete element modelling; Ballasted track; DEM

1. Introduction

An important function of ballast layer is providing sufficient lateral resistance to prevent rail lateral movements. Specifically, the ballast layer provides the lateral resistance to sleeper to resist the forces from the rail thermal elongation (due to temperature change) and excessive axial forces (train loads) [1]. Rail buckling may occur when the lateral resistance of the sleepers is not sufficient, as shown in Figure 1. This issue attracts more attention since the continuous welded rails (CWR) has been widely applied [2]. Lateral CWR buckling is a dangerous phenomenon, which will cause rail and wheel damages and even derailment [3]. The track lateral resistance is utmost important indicator for the track stability and the safety, which helps to quantify the possibility of preventing temp expansion and track buckling [4, 5].

With the increasing of the train speed and axle load, the lateral resistance insufficiency is still an unsolved problem for the traditional ballasted track. For example, the operating train speed in China has increased to 320-360 km/h, and some operating lines even reach the speed 400 km/h. In addition, heavy haul railway

increases the axle loads to above 35 tons [6]. As railway system is developing towards higher speed and heavier axle load, the lateral resistance enhancement is becoming a more and more urgent issue, especially when the vibrational characteristics and resistance-evolution law are considered [7].

Earlier studies have been performed on the ballast bed lateral resistance from the interaction of the ballast and sleeper [8-12] with the Single Sleeper Pull-out Test (SSPT). The SSPT is a widely-used method for measuring ballast bed lateral resistance [13]. Ballast bed lateral resistance is provided primarily by the sleeper-ballast contact interfaces at the base, shoulder ballast and crib ballast [4, 5, 14]. The lateral resistance is considerably dependent on the sleeper characteristics, such as type, weight and spacing [8]. Moreover, it is significantly influenced by the ballast bed properties, such as shoulder ballast size, compaction and degradation stage [14-17]. Based on the effect factors of ballast bed, the optimisation means have been developed in depth, e.g. enlarging the shoulder ballast size, applying steel slag ballast, laying geogrids and spraying ballast glue [5, 11, 18, 19].

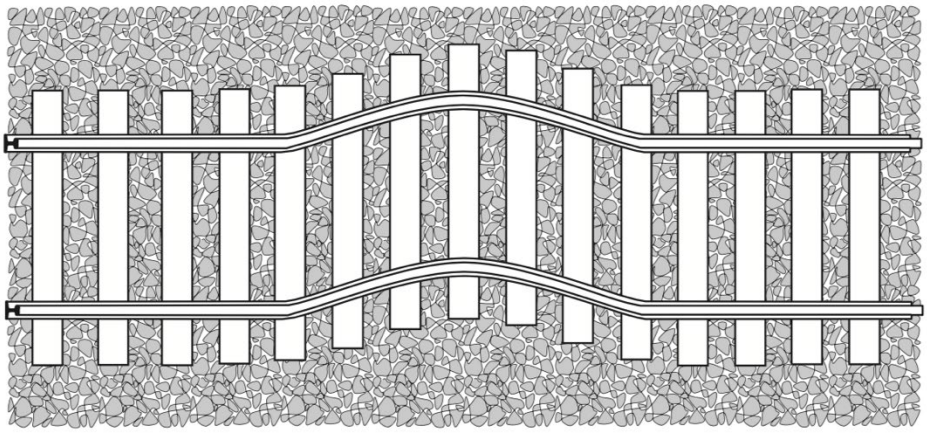

Figure 1 Schematic view of lateral instability of ballasted tracks (figure reproduced from [20])

However, optimization means for the ballast bed have reached a bottleneck due to several reasons. Firstly, the ballast fly (high speed train) limits the ballast bed size. For example, in French railway, the crib ballast is around 6 cm lower than the sleeper, and the shoulder ballast height is reduced. Secondly, tamping and maintenance are difficult for the specific ballast bed (ballast glue or geogrids). Finally, the higher cost of new materials applied in ballast bed is one critical concern. Towards this, sleeper optimisation has become a new better solution and research hot spot to increase the lateral stability of ballasted track.

For instance, in [21], the sleeper shape is designed as mono-block sleeper with wings on the bottom, end side and middle side. From the finite element modelling results, it indicates that winged sleeper can increase the lateral resistance around 50%. In [20], similar optimization was performed and the similar conclusions were draw according to the laboratory tests. Specifically, both sides of sleeper were set two wings making the sleeper “H-shape”. Afterwards, the SSPTs and track panel pull out tests (1:5 scaled) were carried on the H-shape sleepers. In [22], the nailed sleeper is proved as an effective solution that can increase the lateral resistance more than 200%. These studies illustrate that lateral resistance can be enhanced by increasing the contact area of sleeper and ballast bed, however, there are still limitations such as installation difficulty, and tamping maintenance process when applying these kinds of sleepers.

The frictional sleeper makes it possible to increase the lateral resistance without interruption or setback for tamping operations and installation, and the lateral resistance of the frictional sleeper can increase by 64%

as concluded in [16]. The frictional sleeper is the sleeper with its bottom attached with some textures. Many studies evaluated the portion of the base, crib, and shoulder ballast on the lateral resistance (Figure 2) [5, 23-25]. All the studies indicated that the base ballast contributes a majority of lateral resistance, even though the portion results were not similar. For instance, in [5], the contribution of different components (base, crib, and shoulder ballast) are 26–35%, 37–50%, and 15–37%, respectively. In [26], it was proposed the contributions are 45–50, 10–15, and 35–40%, respectively. Therefore, enhancing the sleeper bottom could be an effective means for increasing ballast bed lateral resistance.

In addition, the following advantages of the frictional sleeper can be noted, 1) without influence on sleeper spacing and maintenance operation, 2) less investment in sleeper fabrication and transportation 3) and microscopic interface improvement with ballast particles.

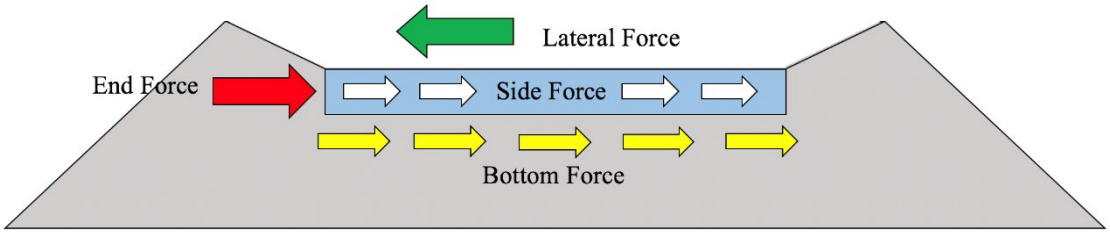

Figure 2 Contribution of the lateral resistance

However, until now, the frictional sleeper studies were performed only with one type of sleeper, and more importantly all the studies were based on the laboratory tests. More types of friction sleeper should be developed to find out the optimal type that can provide the highest lateral resistance. Additionally, before applying the frictional sleeper in the field, the numerical simulations should be performed to check the application feasibility. More importantly, understanding the mesoscopic mechanism (contribution, contact force) of the lateral resistance of frictional sleeper is necessary for further sleeper design. Furthermore, most of the numerical simulations utilised the finite element methods. Limited studies on frictional sleeper were performed with the Discrete Element Method (DEM), which has been demonstrated as an effective tool for railway ballast study e.g. [25, 27-33].

Towards the research gaps, this paper focuses the enhance lateral stability of ballast bed using different types of frictional sleepers (three kinds of bottom texture). The commercial DEM software, Particle Flow Code in three-dimensional is utilised. A set of laboratory SSPTs were performed on the Chinese IIIc type of mono-block concrete sleeper and the three types of frictional sleepers. Based on the test configurations, the DEM ballast bed-sleeper models were built and validated. Based on the DEM models, the effects of bottom texture shape of frictional sleeper to lateral resistance were studied and analysed in mesoscopic level. The results are helpful for further development of sleeper shape towards the track stability enhancement.

2. Laboratory Test

2.1. Materials and Methods

2.1.1. Ballast Bed

The SSPTs were performed upon a 10-meter length ballast bed, and the ballast depth (thickness under

sleepers) is 0.35m with the slope grade at 1:1.75 according to the Chinese ballast bed standard for high speed railway [34]. Firstly, the ballast bed was built in four times by layers (four layers in total), and each layer was compacted 5 times by a vibrating compactor. Afterwards, the track panel was placed on the ballast bed, and ballast were filled in the crib and made the shoulder. Finally, the ballast bed was compacted by vibrating compactor a second time. It should be noted that the sleepers spacing was 600 mm for all tests.

The ballast shoulder height and width are set as different values based on different test configurations (Table 1). In the table, the test number R1-R3 are tests on mono-block sleeper, and the test number A, B and C are tests on the frictional sleeper, which will be introduced in Section 2.1.2.

Traditionally, the ballast shoulder width is supposed to be in the range of 300-500 mm [9]. In addition, it is suggested that an appropriate ballast shoulder width is in the order of 300 mm for conventional ballasted tracks [35], however, the optimal ballast bed size for high speed railway has not been confirmed. Therefore, the SSPTs were performed on different types of sleepers with different dimensions of shoulder width (SW) and shoulder height (SH) as shown in Table 1. It should be noted that crib ballast was filled up to the top level of the sleeper and fully compacted with the vibrator before each test.

Table 1 Single sleeper pull-out test configurations

Test number	Sleeper type	Shoulder width (mm)	Shoulder height (mm)
R1	Mono-block	500	0
R2	Mono-block	500	150
R3	Mono-block	300	0
A1	ST-sleeper	500	0
A2	ST-sleeper	500	150
A3	ST-sleeper	300	0
B1	RT-sleeper	500	0
B2	RT-sleeper	500	150
B3	RT-sleeper	300	0
C1	GT-sleeper	500	0
C2	GT-sleeper	500	150
C3	GT-sleeper	300	0

Table 2 Ballast physical properties of the ballast bed

Property	Standard	Result	Maximum specification value
Micro-Deval loss (%)	BS EN 1097-1	5.20	7.00
Flakiness index (%)	BS EN 93-3	2.20	35.00
Elongation index (%)	BS EN 93-3	0.90	4.00
Fine particle content (%)	BS EN 933-1	0.30	0.60
Fines content (%)	BS EN 93-3	0.20	0.50

The ballast material is basalt that is provided by Tangshan Quarry in Hebei Province. Ballast physical properties were tested according to the British standard, including the durability, mineralogy and particle shape as shown in Table 2. The material is suitable to be used for ballast bed. Additionally, the particle size distribution (PSD) of ballast particles are also according to British standard, as shown in Figure 3 [36].

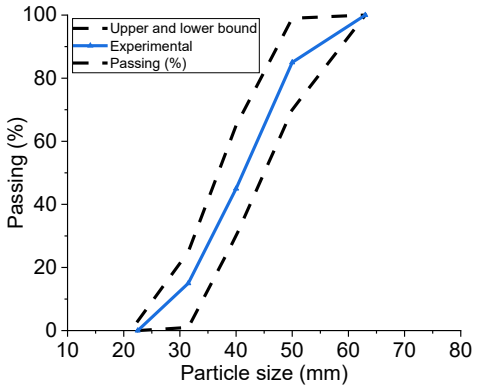

Figure 3 Particle size distribution

2.1.2. Sleepers

Three types of frictional sleepers are designed and produced based on Chinese IIIc mono-block sleeper by attaching texture to the sleeper bottom, as shown in Figure 4. The specifications of the sleepers are as follows: 1) Grooves texture sleeper (GT-sleeper): grooves texture is on the sleeper bottom and the shape of texture block can be found in Figure 4(c). The interval between two blocks is 60 mm. 2) Square texture sleeper (ST-sleeper): this type of sleeper applies the square texture, and the shape of texture block can be found in 3(a). The interval between two blocks is 40 mm. 3) Rhombic texture sleeper (RT-sleeper): the sleeper had rhombic texture, and the shape of texture block is showed in Fig. 3(b). The interval between two blocks is 40 mm.

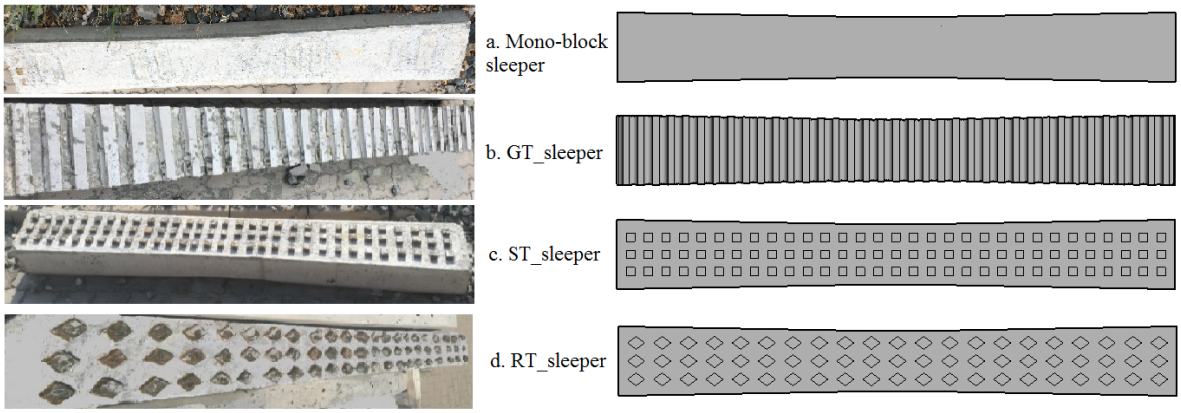

Figure 4 Different types of frictional sleepers: (a) mono-block sleeper, (b) GT-sleeper, (c) ST-sleeper, (d) RT-sleeper

2.1.3. Lateral resistant test setup

The applied test equipment is shown in Figure 5, including the Linear Variable Differential Transformer (LVDT), hydraulic jack, pressure sensor and data acquisition system. The two LVDTs, with the precision at 0.001 mm and measuring range at 0~30 mm, were placed at the sleeper end to measure the lateral displacement of sleepers. The lateral displacement of the sleeper was calculated by the mean value from LVDTs. The hydraulic jack can provide the maximum loading at 10 ton, and the jack actuator stroke is 10 cm, which is long enough to reach the peak resistance value. The hydraulic jack was installed between steel rods and the sleeper end (Figure 5), and the steel rods were used to provide enough resistance. The jack loading was the step-loading that was carried out with 30s intervals. The pressure sensor is with the measuring range at 0~10 ton, and it was placed between the hydraulic jack and the steel rods. Every forces

corresponding to every 2 mm displacements were considered as the lateral resistance of the sleeper. The data acquisition system is IMC, INV3018A that was used to record the resistance force at the sleeper end.

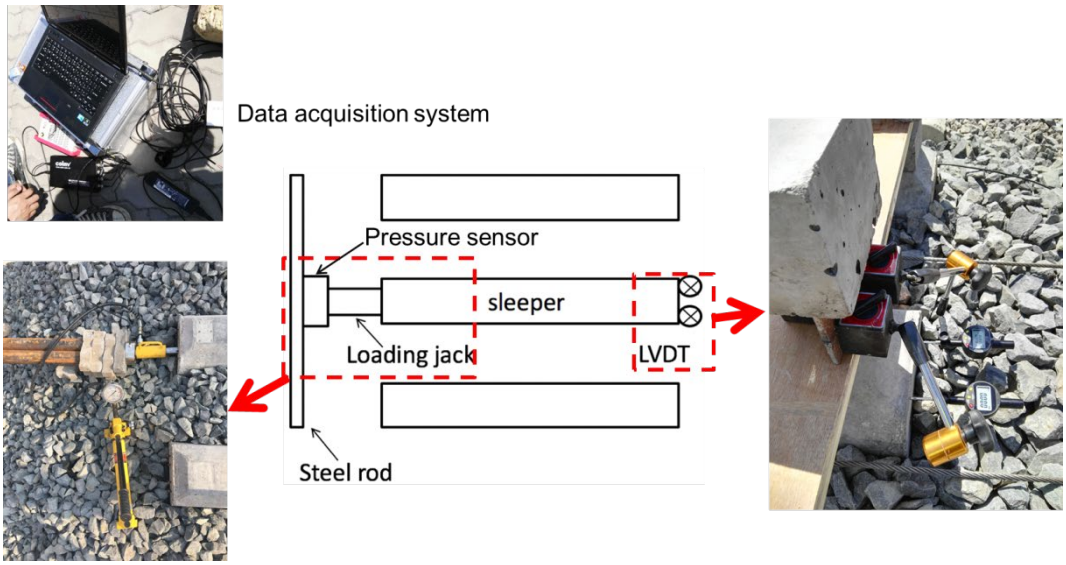

Figure 5 Single sleeper pull-out test setup

2.2. Tests Results

2.2.1. Shoulder height and width

Figure 6 presents the lateral resistance of four types of sleepers at displacement of 2 mm, and it can be seen that the geometry of the ballast bed plays an effective role in the track stability. Specifically, the figure shows that lateral resistance increases significantly with the increase of the shoulder height. In the figure, for example, the SW500_SH150 represents that the shoulder width (SW) is 500 mm and the shoulder height (SH) is 150 mm.

By increasing the shoulder height from 0 to 150 mm (500 mm shoulder width), the resistances of the GT-sleeper, RT-sleeper, ST-sleeper and Mono-block sleeper increase by 23.3%, 27.4%, 24.0% and 33.9%, respectively. In [12], it concluded that the lateral resistance of sleepers increased faintly with the increase of the shoulder width. However, in the presented results, it can be seen that increasing the shoulder width has certain influences on the lateral resistance, which can increase the resistance 11.4% (GT-sleeper), 12.6% (RT-sleeper), 13.8% (ST-sleeper) and 17.4% (mono-block sleeper), respectively.

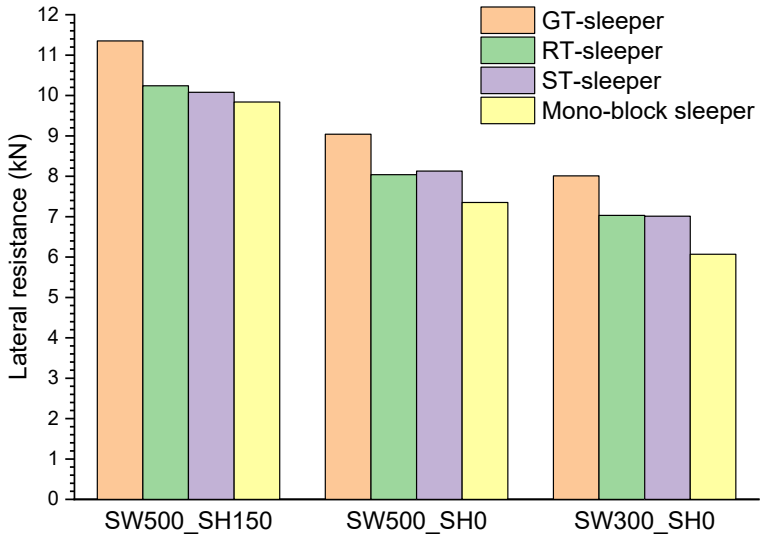

Figure 6 Lateral resistance of four types of sleepers at displacement of 2 mm

2.2.2. Influence of Sleeper types

The lateral resistance of three sleeper types were measured to find the optimal sleeper type. Three types of frictional sleepers are compared with the mono-block sleeper, as shown in Figure 6. From the results, it can be seen that all the frictional sleepers have higher lateral resistance than the mono-block sleeper. Using the GT-sleeper has the lateral resistances at 11.15 kN (SW500_SH150), 9.04 kN (SW500_SH0) and 8.01 kN (SW300_SH0), which are respectively 13.3% and 23.0%, 32.0% higher than the mono-block sleeper resistances. The reason of lateral resistance differences among different types of the frictional sleepers is the different contact forces at the sleeper bottom, which will be demonstrated in the following DEM simulation part.

In addition, according to the test results, it should be noted that the lateral resistance of the RT-sleeper and ST-sleeper are much lower than GT-sleeper. Consequently, the application of GT-sleeper is recommended in ballasted tracks.

3. DEM Simulation

The commercial DEM software, PFC3D, is utilised for the numerical study the frictional sleeper lateral resistance at mesoscopic level. Particularly, the following aspects are studied, including the contribution of different parts (base, crib and shoulder ballast), contact force chain and sleeper bottom interface.

3.1. Model description

3.1.1. Sleeper model

Four types of sleepers were drawn with the AutoCAD, afterwards, according to the drawn sleeper configurations the Wall elements were used to create the sleepers in the PFC3D, as shown in Figure 7(a)-(d).

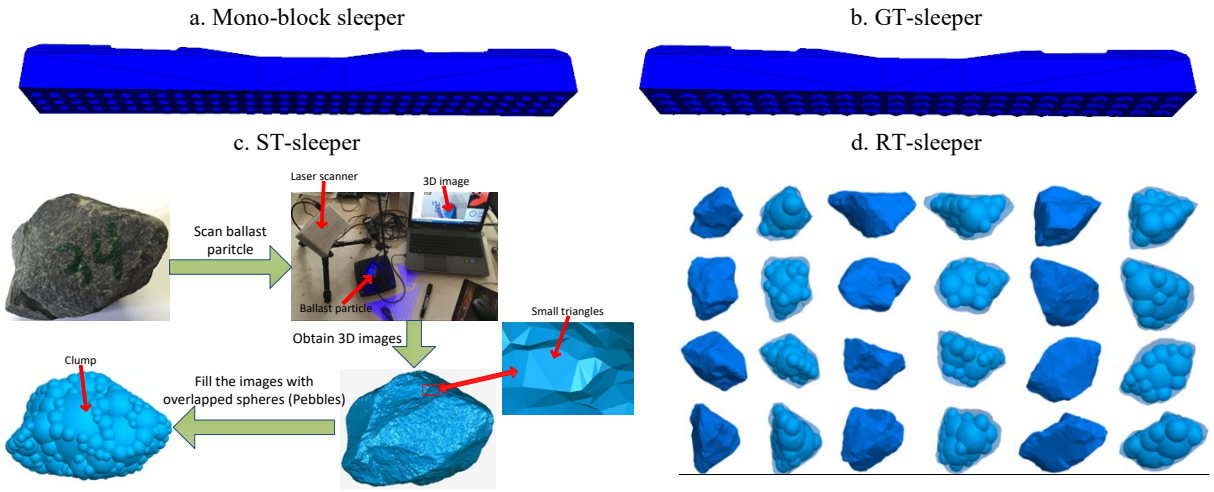

Figure 7 Four types of modelled sleepers and ballast particle generation method

3.1.2. Ballast Particles model

Ballast shape is very important for producing reliable results, and using the digital image correlation technology for ballast particle generation has been widely accepted [37]. The ballast particles in the PFC3D are created with the 3D images that are obtained by laser scanning technique, as shown in Figure 7(e). The 3D images are made of small triangle meshes. Using laser scanning can produce the ballast geometry, and with the geometry the uncrushable particle was generated as the Clump. The Clump is made of spheres (the spheres used to create the Clump are named the Pebble), using the Bubble Pack algorithm of Taghavi [38], as shown in Figure 7(e)(f). The pebble number for making one Clump is in the range of 20-30, and 21 types of Clump are used in the SSPT model.

3.1.3. Contact Model

The linear contact model (LCM) is applied in this study, which needs to define the parameters: normal stiffness, shear stiffness, friction and damping, as shown in Figure 8. In addition, the material parameters should also be defined in the PFC models, i.e. the density. The ballast density is given according to the real density, and the parameters are calibrated according to the experimental results and given in Table 3. The LCM utilises two components (a spring and a dashpot) for kinetic energy transmitting and dissipation at normal and shear directions. The spring provides the no-tension linear elastic force and the shear stiffness together with friction are used to provide shear forces. For the ballast particles, there is no viscos between two ballast particles. Because of this, the dashpot is not active in almost all the earlier studies. The damping applied in the model is the restitution coefficient that is used deciding the particle velocity after acted by a contact force.

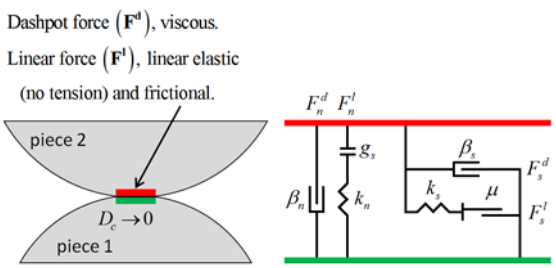

Figure 8 Linear contact model (reproduced from [39])

The spring component is the combination of normal and shear forces (F_l^n; F_l^s), and they can be expressed as shown in Equation 1 [39, 40]. In the equation, the k_n and k_s are the normal and shear stiffness, respectively. The δ_n and $\Delta\delta_s$ are the contact overlap at normal direction and the tangential overlap increment, respectively. The $(F_l^s)_0$ is the previous timestep shear force. The μ is the friction coefficient.

Equation 1

(a) $F_l^n = k_n \delta_n$

(b) $F_{l*}^s = (F_l^s)_0 + k_s \Delta\delta_s$

(c) $F_l^s = \begin{cases} F_{l*}^s & if \quad F_{l*}^s \le \mu F_l^n \\ \mu F_l^n & if \quad F_{l*}^s > \mu F_l^n \end{cases}$

3.1.4. SSPT Model creation

In this section, the SSPT model creation is introduced. The modelled ballast particles (from 3D images) were used to make the ballast bed, and the ballast particles were generated with a self-developed method for faster model creation (introduced later). Before the generation of ballast particles, the sleeper (Wall elements) was generated and fixed at the certain position until the ballast bed stabilised. The detail steps of the model creation are as follows.

Firstly, a profile geometry is created for containing the ballast particles with the Wall command, as shown in Figure 9 (a). The two side walls were made into slopes, which is the same slope grade (1:1.75) as the ballast shoulder.

Afterwards, the spheres are generated in the profile geometry with the same PSD as the experimental tests. The sphere generation keeps on until the required porosity (0.34) is reached. During the generation process, the sleeper is fixed at the certain position. Due to the sphere is randomly generated in the geometry, there are many overlaps between spheres. Therefore, the model should be stabilised with high damping forces until the ratio of unbalanced contact forces to average contact forces is below 0.01. This stage is named the initial equilibrium state.

Finally, the spheres are replaced with Clumps with the self-develop algorithm, which can make that the Clump has the correct volume, density and position. More importantly, the algorithm guarantees a little change at the contact forces between particles. Specifically, as shown in Equation 2, a scaling factor (β) is confirmed based on the contact force. The scaling factor is a factor used to expand the clump size.

Equation 2

(a) $\beta = -1 \cdot \lambda \cdot V_b \cdot \Delta\sigma \cdot k_{sum}^n$

(b) $\Delta\sigma = \sigma_{in} - \sigma_m$

(c) $k_{sum}^n = \sum_i \left(k_i^n \cdot \left(R_i^a + R_i^b\right) \cdot R_i\right)$

In the equation, R_i^a, R_i^b are the radiuses of ith contact between two sphere (a, b); R_i is a constant related with sphere radius and contact; λ is the dimension (3 for 3D); V_b is the ballast bed volume; σ_{in} is the desired stress of ballast bed; σ_m is the current average ballast bed stress; k_i^n is the normal stiffness of the ith contact.

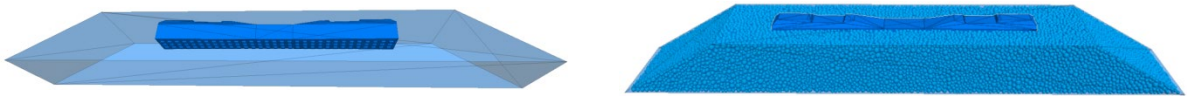

a. Profile geometry

b. Sphere filling in the geometry

c. Replacement and stabilisation

Figure 9 SSPT model creation procedure

3.2. Model validation and calibration

The numerical and experimental results of GT-sleeper are compared for model parameter calibration, due to the GT-sleeper can increase the lateral resistance most. It needs to note that after the SSPT model is created, the sleeper is moved laterally at the speed 0.4 mm/s. As shown in Figure 10, the results of experimental SSPTs are in good agreement with the DEM simulation results. At the displacement of 2 mm, the differences of the results were 2.1% (SW500_SH0), 3.2% (SW500_SH150) and 3.3% (SW300_SH0), respectively. The correlation coefficients are 0.94 (SW500_SH0), 0.94 (SW500_SH150) and 0.96 (SW300_SH0), respectively. The difference is acceptable, and it may be caused by the lack of interlocking of particles. The porosity of the experimental test is difficult to measure. Even though the ballast bed as compacted several times, the compaction is still lower than the DEM model. A set of micro-mechanical parameters adopted for the DEM simulation of ballast can be validated and given in Table 3 based on the comparison results. These parameters will be used in the following simulations.

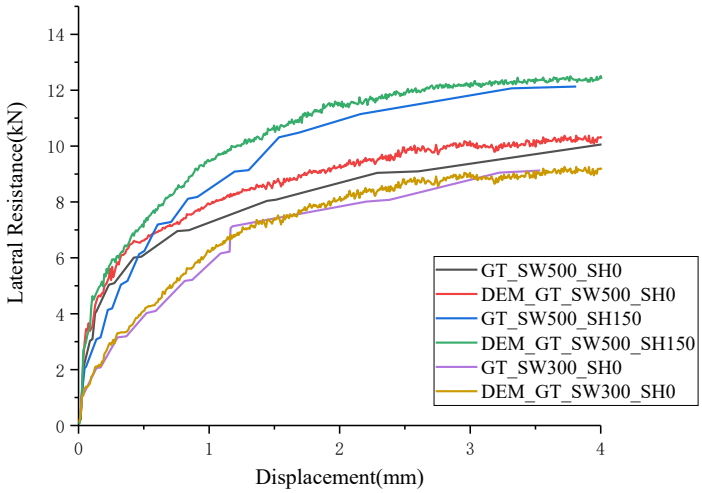

Figure 10 Results of SSPT experimental tests and DEM simulation of GT-sleeper

Table 3 Parameters for the SSPT models

Parameters	Clump	Wall
Normal stiffness, k_n (N/m)	5e9	1e9
Shear stiffness, k_s (N/m)	2e9	1e9
Friction	0.55	0.55
Density (kg/m^3)	2700	-

3.3. Results and discussion

3.3.1. Lateral resistance development

The relationships between lateral resistance and the horizontal displacement of the sleepers obtained from the DEM simulation of SSPTs are shown in Figure 11. From the figure, it can be observed that the lateral resistance increases with and sleeper displacement at the beginning, and after the displacement about 2 mm, the lateral resistance becomes stable.

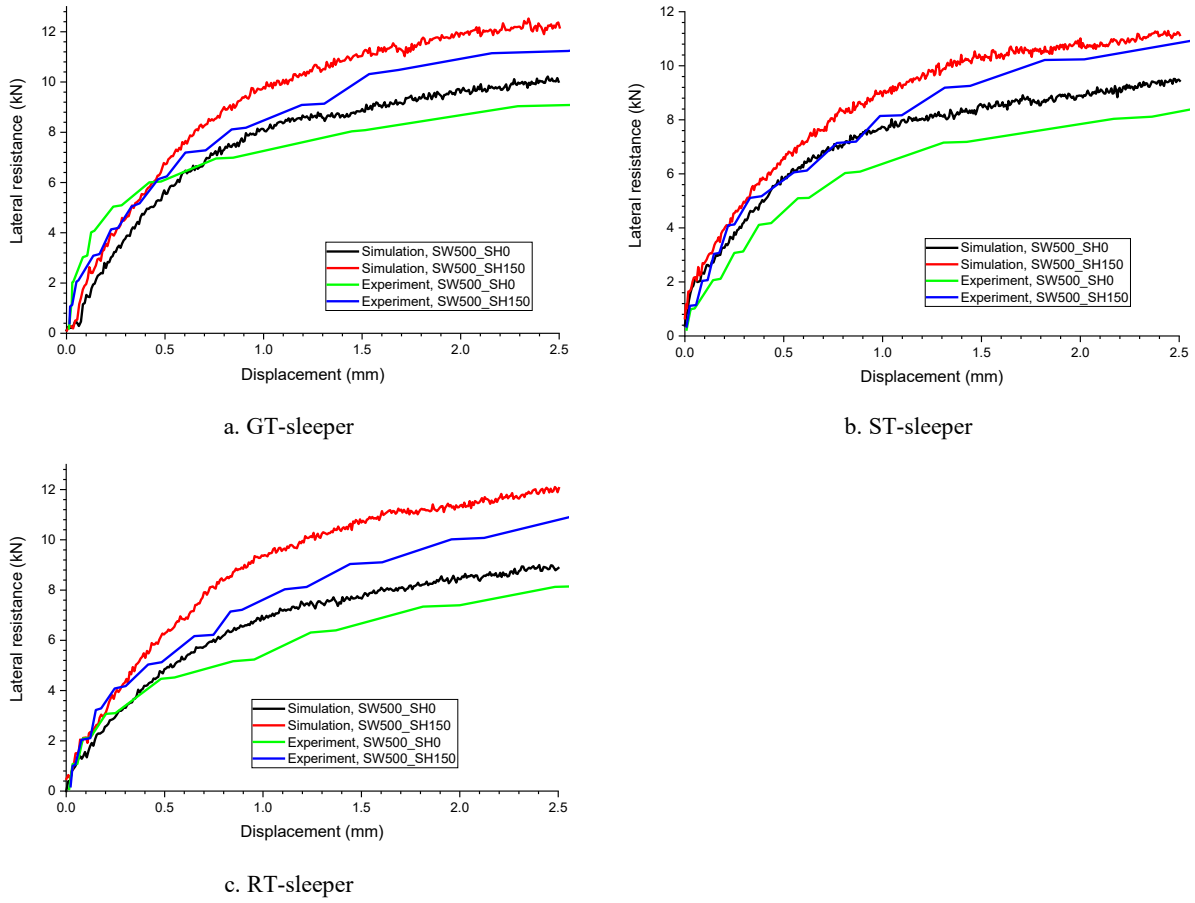

a. GT-sleeper

b. ST-sleeper

c. RT-sleeper

Figure 11 Results of SSPT experimental tests and DEM simulation of three types of frictional sleepers

In addition, all the simulation results are slightly higher than the experimental results. This is due to the field test control is very difficult, especially the compaction, and the DEM model porosity may be a little higher than the experimental test porosity. The difference is within the tolerance and acceptable, and the mesoscopic analysis on the contact force chain, contribution and ballast-sleeper interaction will be performed in the following sections.

3.3.2. Lateral resistance contribution

In Table 4, the contribution of the lateral resistance is given. From the results, the presence of the sleeper bottom texture can increase the base ballast percentage from 37.3% to 52.3% (ST-sleeper), 58.2% (RT-sleeper) and 65.1% (GT-sleeper). This means with the surface texture on the sleeper bottom can increase the lateral resistance at the sleeper bottom. To reveal the mechanism, the contact forces between the sleeper and ballast particles are analysed in the following section.

Table 4 Contribution of different parts for the lateral resistance (SW500_SH0)

Test panel	Base ballast (%)	Crib ballast (%)	Shoulder ballast (%)
Mono-block sleeper	37.3	30.5	32.2
GT-sleeper	65.1	16.3	18.6
ST-sleeper	52.3	23.7	25.0
RT-sleeper	58.2	19.3	22.5

3.3.3. Contact force chain

The contact force chain between the sleeper and ballast particles can show which frictional sleeper is optimal. Figure 12 presents the distribution of contact forces of four types of sleepers. From the figure, it can be observed that using the frictional sleepers can enhance the contacts under the sleeper to provide more lateral resistance. Moreover, the frictional sleepers have smaller contact force chain angle than the normal sleeper, and the GT-sleeper is the optimal one with the smallest angle at 34 degrees. This means more ballast particles can provide forces for the GT-sleeper.

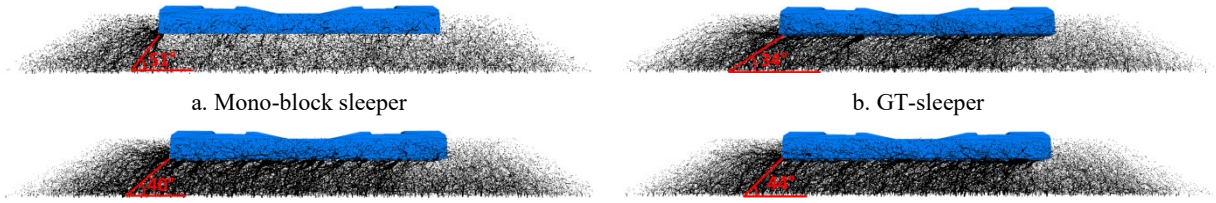

a. Mono-block sleeper b. GT-sleeper

c. ST-sleeper d. RT-sleeper

Figure 12 Contact force chain and distribution of four types of sleepers (SW500_SH0)

3.3.4. Sleeper bottom interface

Table 5 presents the results of four types of sleepers with the shoulder width at 500 mm and height at 0 mm. By comparing the results, it can be concluded that the frictional sleepers have more contact number at the sleeper bottom, 183 (GT-sleeper), 211 (ST-sleeper) and 208 (RT-sleeper) which are at least three times higher than the normal sleeper (61). The contact number increase can be the reason of the lateral resistance increase. The reason of contact number increase is that the bottom texture of frictional sleeper enlarged the effective contact area between sleeper and ballast bed. The enlargement of effective contact area makes the ballast contact number increased at a prominent growing rate.

The average force changes with the type of sleeper, where mono-block sleeper gained the biggest value at 130 N. Although the mono-block sleeper provides the lowest lateral resistance, the contact number of mono-block sleeper is much fewer than frictional sleepers. This leads to higher forces to limited particles. In contrast, the average force of GT-sleeper is small, but its contact number is much more than mono-block sleeper. As a result, the total force of GT-sleeper is the highest.

From the results, it can be concluded that the effect of frictional sleeper can be reflected in two aspects: contact number and average force. By adding bottom texture to the sleeper, the contact number increased significantly while the average force decreased, and the lateral resistance improved eventually. More importantly, the average force decreased when applying the frictional sleepers, which may infer a new method to reduce the stresses at ballast particles for degradation reduction.

Table 5 Contact number and contact force of sleepers

Sleeper type	Mono-block sleeper	GT-sleeper	ST-sleeper	RT-sleeper
Contact number	61	183	211	208
Total force(kN)	7.73	9.33	8.47	8.39
Average force(N)	130	50	40	40

4. Conclusions and perspectives

In this paper, a set of Single sleeper pull-out tests and DEM simulations were performed to study the lateral resistance of normal concrete sleeper (mono-block sleeper) and innovated frictional sleepers (three types). In the experiments, the shoulder ballast height and width were considered as the effect factors. Particularly, the lateral resistance of four types of sleepers were compared to confirm the optimal type. The DEM simulations were used to further analyse the meso-mechanism of ballast-sleeper interaction, revealing the reason of the lateral resistance increase. Based on the results and discussion, the following conclusions are given.

1. Frictional sleepers can increase the lateral resistance. For example, the grooves texture sleeper can increase the resistance by approximately 32.0% compared with traditional concrete sleeper.
2. DEM analysis and results could be served to illustrate the micro-mechanism of ballast-sleeper lateral interaction. Bottom texture of frictional sleeper could provide more contact number, and less average force.
3. The frictional sleepers have better contact force distribution than the traditional sleeper, which means more particles can contribute to the lateral resistance. This leads to the ballasted track more stable.

Acknowledgments

Research was supported by Natural Science Foundation of China (51578051).

References

[1] Hayano K, Koike Y, Nakamura T, Momoya Y. Effects of sleeper shape on lateral resistance of railway ballasted tracks. Advances in Soil Dynamics and Foundation Engineering2014. p. 491-9.
[2] Liu H, Xiao J, Wang P, Liu G, Gao M, Li S. Experimental investigation of the characteristics of a granular ballast bed under cyclic longitudinal loading. Construction and Building Materials. 2018;163(214-24.
[3] Indraratna B, Ngo T. Ballast railroad design: smart-uow approach: CRC Press, 2018.
[4] Kish A. On the fundamentals of track lateral resistance. American Railway Engineering and Maintenance of Way Association. 2011.
[5] Powrie W, Le Pen LM. Contribution of base, crib, and shoulder ballast to the lateral sliding resistance of railway track: a geotechnical perspective. Proceedings of the Institution of Mechanical Engineers, Part F: Journal of Rail and Rapid Transit. 2011;225(2):113-28.
[6] Safari Baghsorkhi M. Experimental investigation of the effect of the ballast/sleeper interventions on railway

track performance: University of Nottingham, 2017.
[7] Liu J, Wang P, Liu G, Xiao J, Liu H, Gao T. Influence of a tamping operation on the vibrational characteristics and resistance-evolution law of a ballast bed. Construction and Building Materials. 2020;239(117879.
[8] Ichikawa T, Hayano K, Nakamura T, Momoya Y. Lateral resistance of ballasted tracks for various shapes of sleepers based on limit equilibrium methods. Japanese Geotechnical Society Special Publication. 2016;2(46):1632-5.
[9] Jing G, Aela P. Review of the lateral resistance of ballasted tracks. Proceedings of the Institution of Mechanical Engineers, Part F: Journal of Rail and Rapid Transit. 2019:095440971986635.
[10] Esmaeili M, Hosseini SAS, Sharavi M. Experimental assessment of dynamic lateral resistance of railway concrete sleeper. Soil Dynamics and Earthquake Engineering. 2016;82(40-54.
[11] Esmaeili M, Zakeri JA, Babaei M. Laboratory and field investigation of the effect of geogrid-reinforced ballast on railway track lateral resistance. Geotextiles and Geomembranes. 2017;45(2):23-33.
[12] Le Pen L, Bhandari AR, Powrie W. Sleeper End Resistance of Ballasted Railway Tracks. Journal of Geotechnical and Geoenvironmental Engineering. 2014;140(5):04014004.
[13] Jing G, Fu H, Aela P. Lateral displacement of different types of steel sleepers on ballasted track. Construction and Building Materials. 2018;186(1268-75.
[14] Bakhtiary A, Zakeri JA, Fang HJ, Kasraiee A. An Experimental and Numerical Study on the Effect of Different Types of Sleepers on Track Lateral Resistance. International Journal of Transportation Engineering. 2015;3(1):7-15.
[15] Zakeri J, Bakhtiary A. Comparing lateral resistance to different types of sleeper in ballasted railway tracks. Scientia Iranica Transaction A, Civil Engineering. 2014;21(1):101.
[16] Zakeri J-A, Mirfattahi B, Fakhari M. Lateral resistance of railway track with frictional sleepers. Proceedings of the Institution of Civil Engineers - Transport. 2012;165(2):151-5.
[17] Nakamura T, Momoya Y, Nomura K, Yoshihiko Y. Shaking Table Test Using Full-scale Model for Lateral Resistance Force of Ballasted Tracks During Earthquake. Procedia Engineering. 2016;143(1100-7.
[18] Jing G, Zhang X, Jia W. Lateral resistance of polyurethane-reinforced ballast with the application of new bonding schemes: Laboratory tests and discrete element simulations. Construction and Building Materials. 2019;221(627-36.
[19] Esmaeili M, Nouri R, Yousefian K. Experimental comparison of the lateral resistance of tracks with steel slag ballast and limestone ballast materials. Proceedings of the Institution of Mechanical Engineers, Part F: Journal of Rail and Rapid Transit. 2016;231(2):175-84.
[20] Koike Y, Nakamura T, Hayano K, Momoya Y. Numerical method for evaluating the lateral resistance of sleepers in ballasted tracks. Soils and Foundations. 2014;54(3):502-14.
[21] Domingo LM, Herraiz JIR, Zamorano C, Herraiz TR. Design of a new high lateral resistance sleeper and performance comparison with conventional sleepers in a curved railway track by means of finite element models. Lat Am J Solids Stru. 2014;11(7):1238-50.
[22] Esmaeili M, Khodaverdian A, Neyestanaki HK, Nazari S. Investigating the effect of nailed sleepers on increasing the lateral resistance of ballasted track. Computers and Geotechnics. 2016;71(1-11.
[23] Kish A, Samavedam G. Track buckling prevention: theory, safety concepts, and applications. John A. Volpe National Transportation Systems Center (US), 2013.
[24] Ciobanu C. Behaviour of the track in hot weather-Rail thermal forces for jointed and CWR track. 2017.
[25] Jing G, Aela P, Fu H. The contribution of ballast layer components to the lateral resistance of ladder sleeper track. Construction and Building Materials. 2019;202(796-805.
[26] Lichtberger B. The lateral resistance of the track (part 2). European Railway Review. 2007.
[27] Irazábal J, Salazar F, Oñate E. Numerical modelling of granular materials with spherical discrete particles and

the bounded rolling friction model. Application to railway ballast. Computers and Geotechnics. 2017;85(220-9.
[28] Tutumluer E, Huang H, Hashash Y, Ghaboussi J. Aggregate shape effects on ballast tamping and railroad track lateral stability. AREMA Annual Conference, Loisville, KY, Sept2006. p. 17-20.
[29] Chen C, Indraratna B, McDowell G, Rujikiatkamjorn C. Discrete element modelling of lateral displacement of a granular assembly under cyclic loading. Computers and Geotechnics. 2015;69(474-84.
[30] Xiao J, Zhang D, Wei K, Luo Z. Shakedown behaviors of railway ballast under cyclic loading. Construction and Building Materials. 2017;155(1206-14.
[31] Li H, McDowell GR. Discrete element modelling of under sleeper pads using a box test. Granular Matter. 2018;20(2).
[32] Harkness J, Zervos A, Le Pen L, Aingaran S, Powrie W. Discrete element simulation of railway ballast: modelling cell pressure effects in triaxial tests. Granular Matter. 2016;18(3):1-13.
[33] Bian X, Li W, Qian Y, Tutumluer E. Micromechanical Particle Interactions in Railway Ballast through DEM Simulations of Direct Shear Tests. International Journal of Geomechanics. 2019;19(5).
[34] China NRAotPsRo. Code for design of high speed railway. TB 1062-2014. 2014.
[35] Li D, Hyslip J, Sussmann T, Chrismer S. Railway geotechnics: CRC Press, 2002.
[36] British Standards Institution BspBE. Aggregates for railway ballast. British Standards Institution London, 2013.
[37] Liu J, Xiao J, Liu H, Liu G, Wang P, Lin Y. Random generation method of ballast 2D topology based on particle characteristics. Construction and Building Materials. 2019;221(762-71.
[38] Taghavi R. Automatic clump generation based on mid-surface. Proceedings, 2nd International FLAC/DEM Symposium, Melbourne2011. p. 791-7.
[39] Itasca C. PFC (particle flow code in 2 and 3 dimensions), version 5.0 [User's manual]. Minneapolis, 2014.
[40] Coetzee C. Calibration of the discrete element method. Powder Technology. 2017;310(104-42.